Neuro-Oncology 12(5):466–472, 2010.
doi:10.1093/neuonc/nop051
Advance Access publication January 22, 2010

Infiltrative patterns of glioblastoma spread detected via diffusion MRI after treatment with cediranib

Elizabeth R. Gerstner, Poe-Jou Chen, Patrick Y. Wen, Rakesh K. Jain, Tracy T. Batchelor, and Gregory Sorensen

Departments of Neurology (E.R.G., T.T.B.), Radiation Oncology (T.T.B., R.K.J.) and Radiology (G.S.), Division of Hematology and Oncology (E.R.G., T.T.B.), Massachusetts General Hospital Cancer Center, Boston, Massachusetts; Center for Neuro-Oncology, Dana-Farber Cancer Institute, Boston, Massachusetts (P.Y.W.); Department of Nuclear Science and Engineering, Massachusetts Institute of Technology, Cambridge, Massachusetts (P.J.C.)

To evaluate the role of apparent diffusion coefficient (ADC) imaging in assessing tumor cell infiltration after treatment with the antivascular endothelial growth factor (anti-VEGF) agent, cediranib, we prospectively analyzed diffusion MRI scans from 30 patients participating in a Phase II trial of cediranib for recurrent glioblastoma. A patient-specific threshold was selected below which ADC values were determined to be abnormally low and suggestive of tumor. We determined the percent of low ADC in the FLAIR hyperintensity surrounding the enhancing tumor and then visualized the location of these low ADC voxels. The percent volume of the FLAIR hyperintensity comprised by low ADC increased significantly from baseline (2.3%) to day 28 (2.9%), day 56 (5.0%), and day 112 (6.3%) of treatment with cediranib suggesting increasing infiltrative tumor in some patients. Visualization of the location of the low ADC voxels suggested regions of tumor growth that were not visible on contrast-enhanced MRI. ADC maps can be used to suggest regions of infiltrative tumor cells with anti-VEGF therapy and should be validated in future studies.

Keywords: ADC, antiangiogenic therapy, diffusion MRI, glioma, infiltration

Drugs that inhibit the vascular endothelial growth factor (VEGF) pathway have shown promising results in early trials of recurrent glioblastoma.[1,2] An emerging problem with anti-VEGF agents, however, is the difficulty in monitoring tumor response to therapy on MRI scans.[3] GBMs are visible on MRI in part because the tumor vasculature is abnormally permeable allowing gadolinium to leak from the intravascular space into the brain parenchyma.[4] Anti-VEGF agents decrease vascular permeability resulting in a decrease in leakage of gadolinium into the brain. Since this regression of contrast enhancement is due primarily to reversal of vascular hyperpermeability, the potential underlying antitumor effect of this class of agents is difficult to ascertain. Preclinical glioma xenograft models treated with anti-VEGF agents have suggested that after an initial period of tumor shrinkage, the tumor starts to grow again by coopting existing native brain blood vessels.[5,6] These native brain blood vessels have an intact blood brain barrier (BBB) so tumor surrounding them is not visible on contrast-enhanced MRI (CE-MRI). Therefore, a better measure than CE-MRI is needed to assess tumor response in the setting of anti-VEGF agents, particularly since these agents are now being combined with cytotoxic drugs.

Magnetic resonance imaging of water diffusion, and particularly apparent diffusion coefficient (ADC) maps, has been proposed as a tool to assess tumor response to treatment.[7–9] Tumors contain areas of increased cell density leading to decreased water diffusion and, thus, low ADC values.[10] Several preclinical and clinical studies have suggested that an increase in ADC values (ie, decrease in cell density) is associated with tumor response to therapy whereas a decrease in ADC (ie, increase in cell density) suggests tumor progression.[7–9,11–14] Consequently, ADC may provide clues about tumor growth or recurrence patterns and prove useful in the assessment of tumor response to

Received March 18, 2009; accepted June 30, 2009.

Corresponding Author: Elizabeth R. Gerstner, MD, Stephen E. and Catherine Pappas Center for Neuro-Oncology, Yawkey 9E, Massachusetts General Hospital, 55 Fruit Street, Boston, MA 02114 (egerstner@partners.org).

anti-VEGF agents. In this study, we investigated tumor escape from cediranib, an oral pan-VEGF receptor tyrosine kinase inhibitor, using ADC. We hypothesized that areas of very low ADC represent growing tumor and that monitoring the change in very low ADC might aid in the interpretation of tumor response in patients with recurrent glioblastoma treated with cediranib.

Materials and Methods

Patients

Diffusion MRI scans were prospectively obtained in 30 patients with recurrent GBM who were enrolled in a National Cancer Institute-sponsored, Phase II clinical trial of cediranib (Clinicaltrials.gov NCT00305656); preliminary findings in 16 of these patients have been previously described.[1] This trial was approved by the institutional review board and patients signed informed consent in order to participate. Two baseline MRI images were acquired prior to initiation of therapy and then on days +1, +28, +56, and +112 after initiation of treatment or until disease progression. Disease progression was determined according to the Macdonald criteria.[15] We also evaluated the change in the volume of FLAIR hyperintensity where a 25% increase (the cut-off used in the Macdonald criteria for contrast-enhancing disease) from the nadir FLAIR volume was considered suggestive of tumor progression.

Diffusion Imaging

Sixty slices of twice refocused echo-planar diffusion weighted images were acquired with TR 4500 ms, TE 84 ms, and a b-value of 700 s/mm^2 in 42 directions as well as 7 low b-value images ($b = 0$ s/mm^2) to allow the diffusion tensor reconstruction at each voxel. Resolution was 2 mm isotropic, with a 128×128 matrix. ADC maps were created from the low and high b-value images using custom written software implementing the standard Steskjal–Tanner diffusion approximation. This provides an estimate of the relative water self-diffusion or water mobility on a voxel-by-voxel basis with higher values representing more water mobility.

K^{trans} Maps

To monitor tumor blood flow and BBB status, dynamic contrast-enhanced MRI data were acquired using a fast gradient echo technique (TR5.7 mS, TE 2.73 ms). The data were processed using custom-made software written in Matlab (The MathWorks, Natick, Massachusetts), following standard published approaches to create maps of K^{trans}, similar to methods previously described.[1]

Image Analysis

Volumetric regions of interest (ROI) were outlined on each patient scan that represented the area of contrast enhancing tumor, the area of abnormal FLAIR hyperintensity (excluding the contrast-enhancing area), the area of adjacent normal brain, and an area of contralateral normal-appearing brain as previously described.[16] For each patient, these ROI were coregistered with the ADC maps using the FSLview tool, FLT (Analysis Group FMRIB, Oxford), in order to determine the values of ADC at each visit within each volumetric ROI.

The baseline (day-1) FLAIR ROI was coregistered to the ADC map of each subsequent visit in order to generate a histogram of the distribution of ADC values within the abnormal baseline FLAIR hyperintensity for each visit. The baseline FLAIR ROI was consistently used across all scan visits since the baseline FLAIR hyperintensity represents the visible extent of potential tumor involvement at diagnosis. The same technique but using the baseline CE ROI was employed to calculate the ADC values within the contrast-enhancing tumor.

To determine abnormally low values of ADC, which would suggest high cell density (ie, tumor), the ADC histogram representing the distribution of ADC values in the contralateral normal-appearing brain at baseline was evaluated for each patient. Two threshold values were picked below which ADC values were deemed abnormally low and thus represented tumor. The first threshold was two standard deviations below the mean value ("subthreshold ADC") and the second was the lowest ADC value seen in normal brain ("subnormal ADC"). We calculated the number of voxels and the percent of the baseline FLAIR (or CE) ROI comprised by subthreshold or subnormal ADC for each patient visit based on their own patient-specific threshold. These voxels with subthreshold or subnormal ADC were then mapped to visualize their location using FSLview.

Statistical Analysis

The two-tailed Wilcoxon test was used to compare the change in the median ADC value on different MRI scan dates as well as the change in subthreshold ADC or subnormal ADC voxels on different study dates. A time-varying Cox proportional hazards model was used to test the univariate association between the percent change in subthreshold or subnormal ADC from baseline (day-1 scan) and progression-free survival (PFS) or overall survival (OS). The percent change in subthreshold or subnormal ADC value was log transformed to achieve the best model fit.

Results

Change in FLAIR Hyperintensity Volume

In all except 2 patients, the volume of FLAIR hyperintensity decreased with cediranib treatment—some as early as day +1 of treatment. The median change in FLAIR volume paralleled the median decrease in the volume of contrast enhancement seen on CE-T1 sequences (Fig. 1). In 7 patients the volume of FLAIR hyperintensity increased over subsequent visits by at

least 25% (range 27%–295%) from nadir volume to the MRI that showed PD or to the last research MRI.

ADC Histograms

Thirty patients were available for ADC histogram analysis at baseline and day 1 of cediranib treatment. Twenty-nine patients were available for analysis on day 28, 19 on day 56, and 14 on day 112. From baseline to day 112, the distribution of ADC values within the baseline FLAIR hyperintensity narrowed with a loss of higher ADC values and the median ADC value shifted significantly to a lower ADC value by 20% ($P < .05$; Fig. 2).

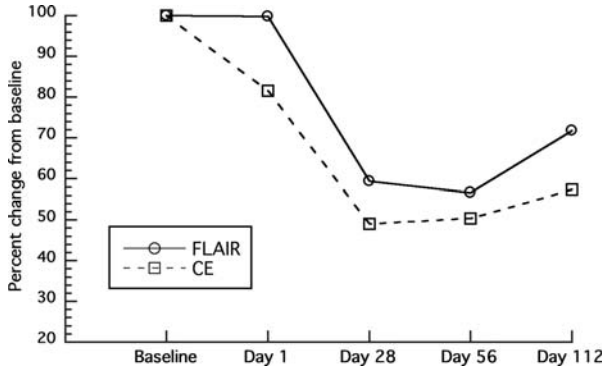

Fig. 1. Median percent change in volume of FLAIR and CE-T1 abnormalities from baseline.

Change in Tumor Volume as Measured by Subthreshold ADC

Following treatment with cediranib, the percent volume of the baseline FLAIR ROI comprised by subthreshold ADC gradually increased. At baseline, 2.3% of the baseline FLAIR ROI was comprised by subthreshold ADC. This percentage increased to 2.9% on day 1 ($P = .32$), 5.0% on day 28 ($P = .0007$), 5.5% on day 56 ($P < .0001$), and 6.3% on day 112 ($P = .0007$) of treatment. The change in volume of subthreshold ADC also increased significantly from baseline to day 1 ($P < .0001$), day 28 ($P < .0001$), day 56 ($P < .0001$), and day 112 ($P < .0002$) of cediranib treatment. This increase in subthreshold ADC (ie, the volume of subthreshold ADC in the area of baseline FLAIR hyperintensity) was associated with a significant reduction in the hazard ratio for progression (HR 0.57, 95% CI 0.34–0.98, $P = .04$) and with a trend towards improvement in OS that did not reach statistical significance (HR 0.69, 95% CI 0.41–1.14, $P = .144$). The percentage of subthreshold ADC voxels did not change significantly in the area in the contralateral normal-appearing brain.

Change in Tumor Volume as Measured by Subnormal ADC

In order to exclude any potential overlap with normal brain, we also evaluated an ADC threshold that was below the lowest value in normal-appearing brain (subnormal ADC). Following treatment with cediranib, the

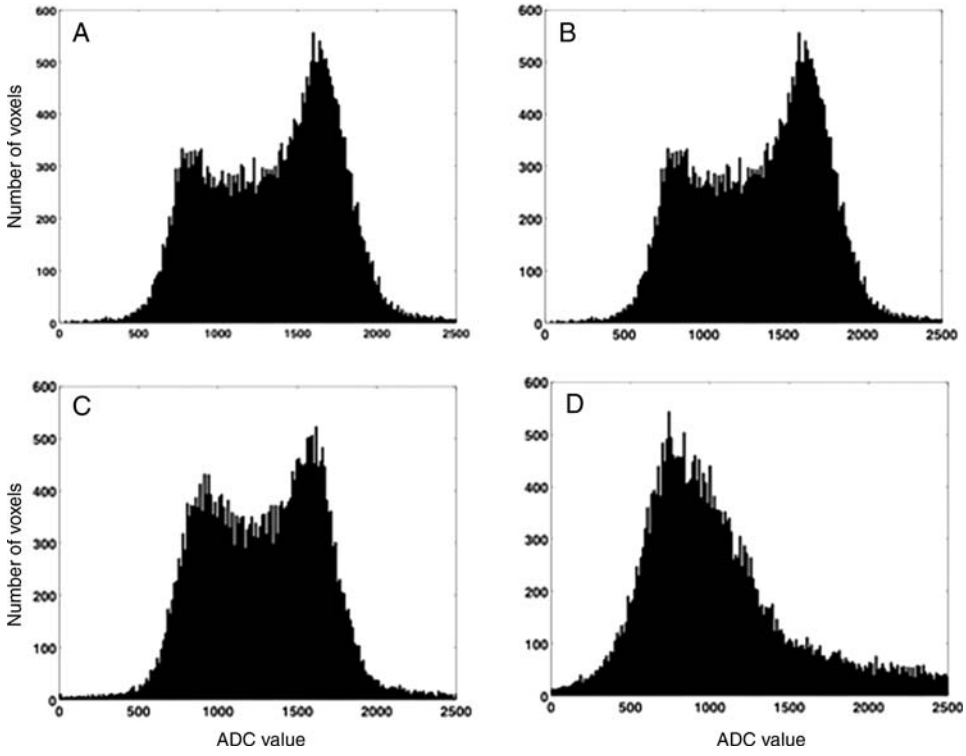

Fig. 2. Sample ADC histogram from one patient showing the distribution of ADC values within the baseline FLAIR hyperintensity. (A) baseline ADC histogram (B) day +1 ADC histogram (C) day +28 ADC histogram (D) day +56 ADC histogram. ADC values are $\times 10^{-6}$ mm^2/s.

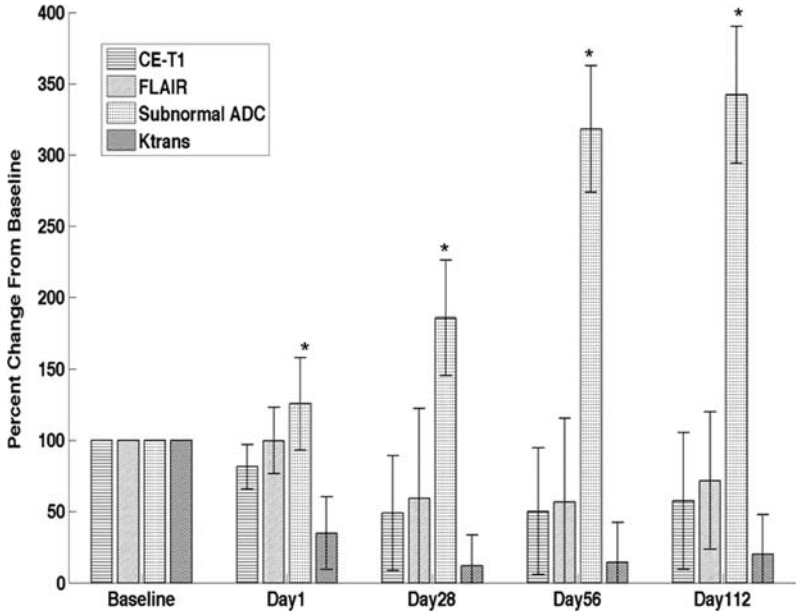

Fig. 3. Percent change from baseline of contrast-enhancing tumor volume (CE-T1), FLAIR hyperintensity volume, median K^{trans} value within the contrast-enhancing tumor, and percent volume of subnormal ADC within the baseline FLAIR hyperintensity. * indicates a statistically significant change from baseline ($P < .05$). Bars indicate standard deviation.

percent volume of the baseline FLAIR ROI comprised by subnormal ADC also gradually increased. At baseline, 1.1% of the baseline FLAIR ROI was comprised by subnormal ADC. This percentage increased to 1.5% on day 1 ($P = .27$), 2.4% on day 28 ($P = .0054$), 2.4% on day 56 ($P = .0015$), and 3.1% on day 112 ($P = .0027$) of treatment. The percent change in volume of subnormal ADC within the baseline FLAIR ROI increased significantly from baseline to day 1 ($P < .0001$), day 28 ($P < .0001$), day 56 ($P < .0001$), and day 112 ($P < .0001$) of cediranib treatment (Fig. 3). The association with survival was less robust when using the subnormal cutoff compared with the subthreshold cutoff but was still suggestive for prolonged PFS (HR 0.40, 95% CI 0.15, 1.08, $P = .07$) and OS (HR 0.49, 95% CI 0.18, 1.32, $P = .16$).

Vascular Permeability

K^{trans}, a measure of combined tumor flow/vascular permeability, dropped significantly by day 28 and remained low at day 112 suggesting that changes in BBB permeability and continued fluid exchange could not account for the change in subthreshold or subnormal ADC values (Fig. 3).

Location of Subthreshold and Subnormal ADC

The location within the baseline FLAIR hyperintensity with subthreshold and subnormal ADC voxels was mapped. The location of subthreshold and subnormal ADC remained consistent within patients from one visit to the next. In 19 and 23 patients, there was an absolute increase in the percent of subthreshold and subnormal ADC, respectively, from baseline to last research MRI scan. In most of these patients, the location of the subthreshold and subnormal ADC clustered together suggesting an island of growing tumor (Fig. 4). In the remaining patients, there was no obvious clustering of ADC to suggest infiltrative tumor cells.

Discussion

In a subset of patients with recurrent GBM treated with cediranib, we demonstrate that the volume of subthreshold ADC in the baseline FLAIR hyperintensity significantly increases over serial MRI scans. Since the ADC value is inversely correlated with tissue cellularity, this increase in the volume of subthreshold ADC abnormality may reflect an increase in the volume of the infiltrative tumor that is not detected on conventional CE-MRI scans.[7,9] Our data confirm several preclinical mouse glioma models that suggested that blocking VEGF leads to a more infiltrative pattern of tumor growth.[5,6,17,18] When angiogenesis is blocked, tumor cells grow along existing brain blood vessels in a process termed vascular cooption in order to maintain an adequate tumor blood supply.

Our data also confirm earlier human studies suggesting tumor growth after anti-VEGF treatment. In humans treated with anti-VEGF therapy, changes on MRI T2/FLAIR sequences have been suggested to represent vascular cooption.[19] However, an increase in FLAIR signal can also reflect gliosis from prior treatments, vascular disease, or cerebral edema. In our cohort of patients, the volume of FLAIR hyperintensity decreased in the majority of patients likely because of the antiedema effect of cediranib. Changes in the volume of FLAIR hyperintensity paralleled changes in

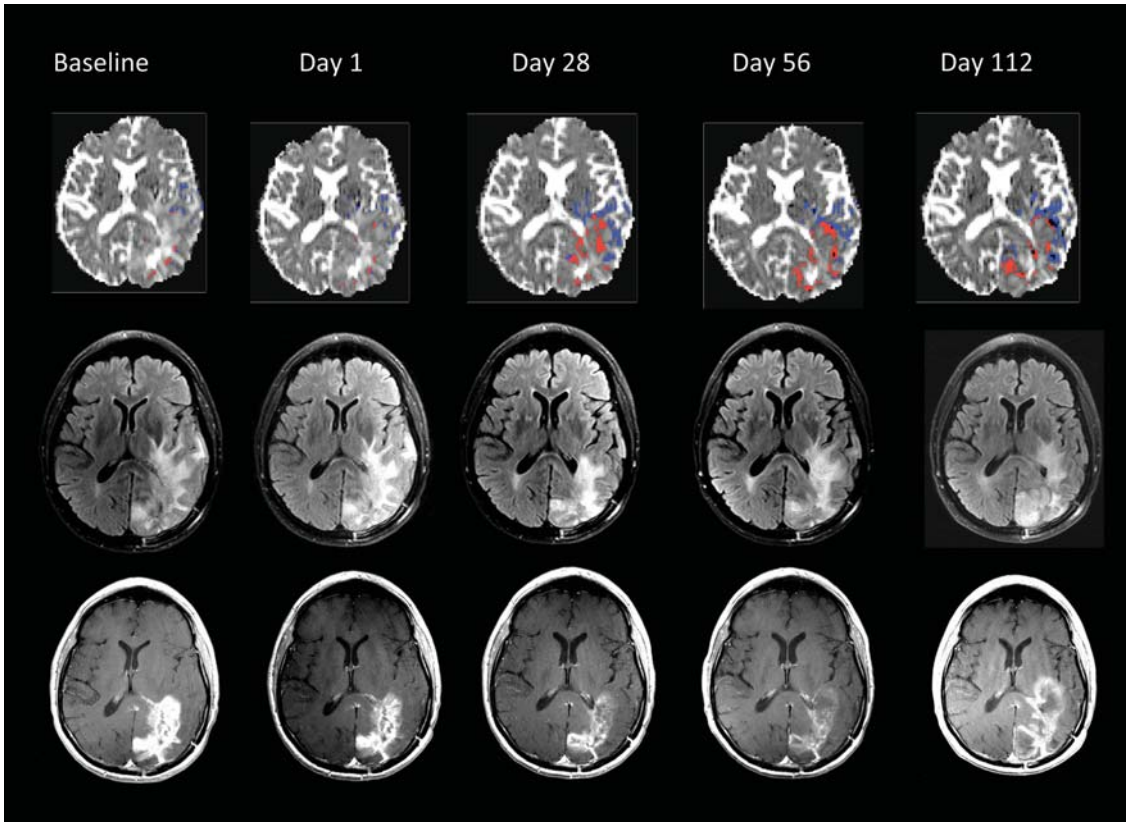

Fig. 4. Location of subnormal ADC in a representative patient with increasing subnormal ADC. Red indicates subnormal ADC within baseline contrast-enhanced ROI. Blue indicates subnormal ADC within baseline FLAIR ROI. ADC images (top row); FLAIR images (middle row); post-contrast T1 images (bottom row).

contrast enhancement in the majority of patients so added little value to detecting early tumor growth. On the other hand, ADC is more quantifiable, less subjective to measuring error, and potentially more specific in determining tumor growth or relapse. Our results extend previous work by using ADC as an alternative to FLAIR volume or contrast enhancement and provides evidence in humans that supports the notion of vascular cooption as a tumor breakthrough mechanism.

The utility of ADC in the setting of anti-VEGF therapy has not been previously studied in humans or animals with gliomas. Thoeny et al.[11] studied the tubulin inhibitor, combretastatin A4 phosphate, which disrupts endothelial cells in an animal model of rhabdomyosarcoma. The investigators demonstrated that ADC initially decreased after injection of combretastatin, then increased as histologically confirmed necrosis occurred, and finally decreased again as the tumor progressed. Physiologically, this might correlate with the agent reducing vasogenic edema followed by tumor cell killing (necrosis and increased water mobility) and then tumor escape and growth. In our study, we were unable to detect the initial increase in ADC observed in the animal models but were able to detect the increase in low ADC suggestive of a pattern of infiltrative tumor growth. This increase in infiltrative tumor growth, however, was associated with prolonged PFS suggesting a less aggressive phenotype for infiltrative tumors. One hypothesis could be that anti-VEGF agents slow the growth of more destructive tumors and make them behave like lower grade gliomas so there is longer preservation of appropriate neuronal function.

Deciding what threshold ADC value to choose for determining tumor vs nontumor is complicated. For this reason, we tested 2 patient-specific possibilities, 1 that was 2 standard deviations below the mean value in normal brain and the second that was below the lowest value in normal brain. Reassuringly, both of these thresholds provided similar results and future studies should continue to refine the precise, patient-specific threshold necessary to identify tumor with diffusion imaging.

Our results build on, but are distinct from, prior pioneering studies of ADC in brain tumor patients in which ADC was evaluated as an early predictor of tumor response to conventional cytotoxic therapy rather than as a tool to study tumor relapse patterns.[20–24] By capitalizing on the quantitative nature of ADC, we were able to suggest the location of populations of tumor cells. Precise visualization of the location of tumor burden sheds light on tumor migration and recurrence patterns and highlights the heterogeneous nature of glioma growth. Further work, and especially histological confirmation, needs to be done to verify whether or not ADC can be used in humans to detect tumor escape via infiltration and vascular cooption.[5,6]

One clear limitation of utilizing ADC to assess for infiltrative tumor is that changes in ADC can be related to different physiological processes that restrict diffusion of water. We took a number of measures to maximize the tumor specificity of our ADC measurements. For example, the most common cause of decreased ADC is ischemia but this was an unlikely explanation in our patient cohort since follow-up imaging repeatedly demonstrated no evidence of infarction in any patient. Alternately, resolution of edema, a known effect of the anti-VEGF agents, may decrease ADC values.[1] Within an MRI voxel, edema, normal brain, and infiltrating tumor all contribute to the calculation of the ADC value for that voxel. Therefore, an increase in the volume of low ADC voxels could partially represent the resolution of vasogenic edema. To avoid this problem we chose a patient-specific threshold value of ADC that was so low, we postulate it was unlikely to be confounded by edema. By choosing ADC values that are low even for normal brain, much less edematous brain, the contribution of edema is minimized, thus, increasing the likelihood that our very-low ADC voxels only represented infiltrating tumor cells. In addition, K^{trans}, a measure of flow/BBB permeability, did not change significantly after day 28, which is when we saw much of the change in the volume of low ADC tissue, suggesting that it is unlikely that further significant decreases in edema occurred after this time point that might confound our results. Therefore, although further studies are needed, we anticipate that several MRI techniques, including diffusion imaging, will prove useful in assessing GBM response to this class of agents.

Funding

This work was supported by R01CA129371-01 (Batchelor) and M01-RR-01066, National Institutes of Health, National Center for Research Resources, General Clinical Research Centers Program.

Conflict of interest statement. None declared.

References

1. Batchelor TT, Sorensen AG, di Tomaso E, et al. AZD2171, a pan-VEGF receptor tyrosine kinase inhibitor, normalizes tumor vasculature and alleviates edema in glioblastoma patients. *Cancer Cell.* 2007;11:83–95.
2. Cloughesy TF, Prados MD, Wen PY, et al. A phase II, randomized, non-comparative clinical trial of the effect of bevacizumab (BV) alone or in combination with irinotecan (CPT) on 6-month progression free survival (PFS6) in recurrent, treatment-refractory glioblastoma (GBM). *J Clin Oncol.* 2008; 26 (suppl): abstract 2010b.
3. Sorensen AG, Batchelor TT, Wen PY, Zhang WT, Jain RK. Response criteria for glioma. *Nat Clin Pract Oncol.* 2008;5:634–644.
4. Hesselink JR, Press GA. MR contrast enhancement of intracranial lesions with Gd-DTPA. *Radiol Clin North Am.* 1988;26:873–887.
5. Rubenstein JL, Kim J, Ozawa T, et al. Anti-VEGF antibody treatment of glioblastoma prolongs survival but results in increased vascular cooption. *Neoplasia.* 2000;2:306–314.
6. Kunkel P, Ulbricht U, Bohlen P, et al. Inhibition of glioma angiogenesis and growth in vivo by systemic treatment with a monoclonal antibody against vascular endothelial growth factor receptor-2. *Cancer Res.* 2001;61:6624–6628.
7. McConville P, Hambardzumyan D, Moody JB, et al. Magnetic resonance imaging determination of tumor grade and early response to temozolomide in a genetically engineered mouse model of glioma. *Clin Cancer Res.* 2007;13:2897–2904.
8. Hall DE, Moffat BA, Stojanovska J, et al. Therapeutic efficacy of DTI-015 using diffusion magnetic resonance imaging as an early surrogate marker. *Clin Cancer Res.* 2004;10:7852–7859.
9. Chenevert TL, Stegman LD, Taylor JM, et al. Diffusion magnetic resonance imaging: an early surrogate marker of therapeutic efficacy in brain tumors. J Natl Cancer Inst. *2000*;92:2029–2036.
10. Chenevert TL, Sundgren PC, Ross BD. Diffusion imaging: insight to cell status and cytoarchitecture. *Neuroimaging Clin N Am.* 2006;16: 619–632, viii–ix.
11. Thoeny HC, De Keyzer F, Chen F, et al. Diffusion-weighted MR imaging in monitoring the effect of a vascular targeting agent on rhabdomyosarcoma in rats. *Radiology.* 2005;234:756–764.
12. Lee KC, Hall DE, Hoff BA, et al. Dynamic imaging of emerging resistance during cancer therapy. *Cancer Res.* 2006;66:4687–4692.
13. Lazovic J, Jensen MC, Ferkassian E, Aguilar B, Raubitschek A, Jacobs RE. Imaging immune response in vivo: cytolytic action of genetically altered T cells directed to glioblastoma multiforme. *Clin Cancer Res.* 2008;14:3832–3839.
14. Chenevert TL, McKeever PE, Ross BD. Monitoring early response of experimental brain tumors to therapy using diffusion magnetic resonance imaging. *Clin Cancer Res.* 1997;3:1457–1466.
15. Macdonald DR, Cascino TL, Schold SC, Jr, Cairncross JG. Response criteria for phase II studies of supratentorial malignant glioma. *J Clin Oncol.* 1990;8:1277–1280.
16. Sorensen AG, Patel S, Harmath C, et al. Comparison of diameter and perimeter methods for tumor volume calculation. *J Clin Oncol.* 2001;19:551–557.
17. Gomez-Manzano C, Holash J, Fueyo J, et al. VEGF Trap induces antiglioma effect at different stages of disease. *Neuro Oncol*. 2008; 10:940–945.
18. Jain RK, di Tomaso E, Duda DG, Loeffler JS, Sorensen AG, Batchelor TT. Angiogenesis in brain tumours. *Nat Rev Neurosci*. 2007;8: 610–622.
19. Norden AD, Young GS, Setayesh K, et al. Bevacizumab for recurrent malignant gliomas: efficacy, toxicity, and patterns of recurrence. *Neurology*. 2008;70:779–787.
20. Mardor Y, Pfeffer R, Spiegelmann R, et al. Early detection of response to radiation therapy in patients with brain malignancies using conventional and high *b*-value diffusion-weighted magnetic resonance imaging. *J Clin Oncol.* 2003;21:1094–1100.

21. Mardor Y, Roth Y, Lidar Z, et al. Monitoring response to convection-enhanced taxol delivery in brain tumor patients using diffusion-weighted magnetic resonance imaging. *Cancer Res.* 2001;61: 4971–4973.
22. Hamstra DA, Galban CJ, Meyer CR, et al. Functional diffusion map as an early imaging biomarker for high-grade glioma: correlation with conventional radiologic response and overall survival. *J Clin Oncol.* 2008;26:3387–3394.
23. Hamstra DA, Chenevert TL, Moffat BA, et al. Evaluation of the functional diffusion map as an early biomarker of time-to-progression and overall survival in high-grade glioma. *Proc Natl Acad Sci USA.* 2005;102:16759–16764.
24. Moffat BA, Chenevert TL, Lawrence TS, et al. Functional diffusion map: a noninvasive MRI biomarker for early stratification of clinical brain tumor response. *Proc Natl Acad Sci USA.* 2005;102: 5524–5529.